

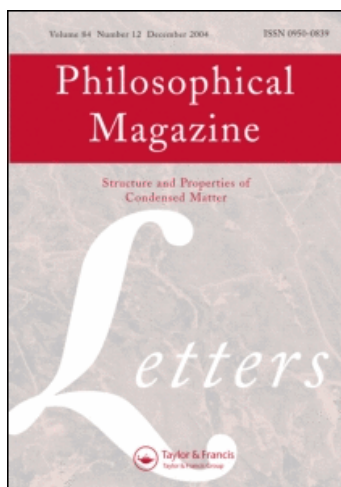
This article was downloaded by: [Imperial College]

On: 7 January 2010

Access details: Access Details: [subscription number 908039594]

Publisher Taylor & Francis

Informa Ltd Registered in England and Wales Registered Number: 1072954 Registered office: Mortimer House, 37-41 Mortimer Street, London W1T 3JH, UK



Philosophical Magazine Letters

Publication details, including instructions for authors and subscription information:

<http://www.informaworld.com/smpp/title~content=t713695410>

A simple model for large-scale simulations of fcc metals with explicit treatment of electrons

D. R. Mason ^a; W. M. C. Foulkes ^a; A. P. Sutton ^a

^a Department of Physics, Imperial College London, London, SW7 2AZ, UK

Online publication date: 02 December 2009

To cite this Article Mason, D. R., Foulkes, W. M. C. and Sutton, A. P.(2010) 'A simple model for large-scale simulations of fcc metals with explicit treatment of electrons', Philosophical Magazine Letters, 90: 1, 51 – 60

To link to this Article: DOI: 10.1080/09500830903430979

URL: <http://dx.doi.org/10.1080/09500830903430979>

PLEASE SCROLL DOWN FOR ARTICLE

Full terms and conditions of use: <http://www.informaworld.com/terms-and-conditions-of-access.pdf>

This article may be used for research, teaching and private study purposes. Any substantial or systematic reproduction, re-distribution, re-selling, loan or sub-licensing, systematic supply or distribution in any form to anyone is expressly forbidden.

The publisher does not give any warranty express or implied or make any representation that the contents will be complete or accurate or up to date. The accuracy of any instructions, formulae and drug doses should be independently verified with primary sources. The publisher shall not be liable for any loss, actions, claims, proceedings, demand or costs or damages whatsoever or howsoever caused arising directly or indirectly in connection with or arising out of the use of this material.

A simple model for large-scale simulations of fcc metals with explicit treatment of electrons

D.R. Mason*, W.M.C. Foulkes and A.P. Sutton

Department of Physics, Imperial College London, London, SW7 2AZ, UK

(Received 7 May 2009; final version received 29 July 2009)

The continuing advance in computational power is beginning to make accurate electronic structure calculations routine. Yet, where physics emerges through the dynamics of tens of thousands of atoms in metals, simplifications must be made to the electronic Hamiltonian. We present the simplest extension to a single s-band model [A.P. Sutton, T.N. Todorov, M.J. Cawkwell and J. Hoekstra, *Phil. Mag. A* 81 (2001) p.1833.] of metallic bonding, namely, the addition of a second s-band. We show that this addition yields a reasonable description of the density of states at the Fermi level, the cohesive energy, formation energies of point defects and elastic constants of some face-centred cubic (fcc) metals.

Keywords: tight-binding; transition metal; computer simulation; electronic structure; point defects

1. Introduction

Where the physics of metals requires an accurate description of the electronic structure, the first choice of simulation methods is often density functional theory (DFT). For some transition and noble metals, there are good d-band or s–p–d-band tight binding (TB) models available, which are significantly less computationally expensive than DFT techniques, and yet retain an explicit treatment of electronic relaxation as atoms are displaced [1]. However, there are many examples in the physics of metals, which are of great practical significance, that require a treatment of the dynamics of thousands or millions of atoms, over time scales that are too large even for such TB models to be used with current computing resources. In such cases, it is common practice to use instead an effective interatomic potential in which electrons appear only implicitly through the choice of the function of the atomic positions that defines the potential. Whenever an interatomic potential is used, the Born–Oppenheimer approximation is made – it is assumed that as the response of electrons is sufficiently fast, they can relax into their ground state wherever the nuclei go. In that case, the energy of the system depends only on the atomic coordinates. The approximation breaks down when electrons are excited. For example, the large atomic velocities created by high-energy impacts of massive particles during

*Corresponding author. Email: daniel.mason@imperial.ac.uk

irradiation or sputtering excite electrons out of their ground states. But there are very few TB models which are sufficiently simple to allow one to treat the dynamics of thousands or millions of atoms in a metal over time scales of molecular dynamics simulations comparable to those accessible with simple interatomic potentials.

Sutton et al. [2] described the simplest possible TB model in which a single s-band description of valence electrons is fitted to certain properties of noble metals. This model has been used to explore the physics of electromigration in nanowires [3], current induced heating in nanowires [4], and electronic excitations and their influence on interatomic forces in radiation damage [5,6]. In each of these applications, the simplicity of the model has enabled the physics to be explored in systems that were considered too large to be modelled by a more accurate electronic Hamiltonian. In polymer physics, a single s-band model has also been used with great success. The Su–Schrieffer–Heeger (SSH) model of polyacetylene [7] has been used extensively to model electron–phonon coupling in a model conjugated polymer. We contend that in any atomistic simulation there will always have to be a balance struck between the accuracy of a model defined in terms of (a) the treatment of electronic relaxation and dynamics, and (b) the number of atoms and the period of time that can be simulated. As computing power increases, the need for the balance will never be removed; it will only move the fulcrum towards the treatment of ever larger systems and longer periods of time. Similarly, it will always be the case that the largest systems and longest periods of time will be simulated only with interatomic potentials, and there will always be a demand for improved potentials, irrespective of the advances in simulations based on DFT or TB descriptions of atomic interactions.

The simple model described in [2] is unable to capture features that have turned out to be significant in some materials processes. The density of states at the Fermi level is not well described. Moreover, as the bandfilling was selected as a fitting parameter, the effective nuclear charges on atoms are non-integer. The aim of this article is to make the simplest possible modification to the single s-band model, which will remove these limitations with the minimum increase of computational cost. Our model aims to reproduce the correct low-temperature crystal structure, the elastic properties and cohesive energy, together with the density of states at the Fermi level and integer charge states of isolated atoms. We achieve this by adding a second s-orbital.

The second orbital is not intended to replace the d-band, which is known to be crucial for the correct description of directional bonding in a transition metal [8]. It merely provides sufficient flexibility to approximate the correct density of states at the Fermi level while retaining mechanical stability. In this sense, a parallel can be drawn with the very successful Vogl sp^3s^* basis set for silicon, where the higher energy s^* orbital adds significantly to the flexibility and transferability of the model without undue increase in complexity [9]. We have found that the fitting process naturally makes the second orbital narrower, and placed relative to the Fermi level in such a way as to mimic the position of the d-band. The density of states produced thus have features similar to those of transition metals. The model proposed here suffers from the absence of some directional bonding with any s-band model, but with the improvements to the density of states at the Fermi energy, the overall shape of the density of states and the number of electrons per atom make it significantly more suitable for some applications. These include, for example, studying the

influence of the density of states at the Fermi energy on current-induced effects in nanowires and on electronic excitation in radiation damage in metals.

2. A two orbital tight-binding model

Our starting point is the single s-band model of [2]. This model has five adjustable parameters: an energy scale ϵ , a measure of the hopping integral strength c , repulsive and hopping exponents p and q and bandfilling ν . These are fitted in turn to the cohesive energy, lattice parameter a and bulk modulus, leaving some flexibility for best fitting the other elastic moduli by tuning the bandfilling subject to the constraint that the face-centred cubic (fcc) structure is most stable. The hopping integral between atoms m and n is given by

$$H_{mn} = H(R_{mn}) \equiv H(|\mathbf{R}_m - \mathbf{R}_n|) = -\frac{\epsilon c}{2} \left(\frac{a}{R_{mn}} \right)^q \quad (1)$$

for $m \neq n$, and zero otherwise. The binding energy of atom n in a neutral bulk crystal in this model is then a sum of a repulsive pairwise interaction and the electronic bond energy:

$$E_B = \frac{\epsilon}{2} \sum_{m \neq n} \left(\frac{a}{R_{mn}} \right)^p + 2 \sum_{m \neq n} H_{nm} \rho_{mn}, \quad (2)$$

where R_{mn} is the distance between atoms m and n and ρ_{mn} , the bond order between them. The factor 2 is for spin degeneracy.

We generalise this model to two s-orbitals, which we label s and s^* , by making the adjustable parameters c and q symmetric 2×2 matrices \mathbf{c} and \mathbf{q} . We also shift the s - and s^* -bands relative to each other to allow for different first moments. The hopping integral coupling orbital α on atom m with orbital β on atom n , with α, β being s or s^* , is then

$$H_{mn}^{\alpha\beta}(R_{mn}) = \begin{cases} -\frac{\epsilon c^{\alpha\beta}}{2} \left(\frac{a}{R_{mn}} \right)^{q^{\alpha\beta}}, & m \neq n \\ E_s, & m = n, \alpha = \beta = s \\ E_{s^*}, & m = n, \alpha = \beta = s^* \\ 0, & m = n, \alpha \neq \beta. \end{cases} \quad (3)$$

The repulsive pairwise potential will take the same form as in Equation (2). We terminate both repulsive and hopping integral contributions using the smooth polynomial scheme described in Appendix A. We apply the termination between the positions of the second- and third-nearest neighbours in the perfect fcc crystal.

Assuming that the system is not spin polarised, the binding energy of atom n in the s - s^* model is then

$$E_B = \frac{\epsilon}{2} \sum_{m \in \mathcal{N}_n} \left(\frac{a}{R_{mn}} \right)^p + 2 \sum_{m \in \mathcal{N}_n} \sum_{\alpha\beta} H_{nm}^{\alpha\beta} \rho_{nm}^{\beta\alpha} + 2 \sum_{\alpha\beta} H_{nn}^{\alpha\beta} \rho_{nn}^{\beta\alpha} - E_{at}, \quad (4)$$

where \mathcal{N}_n indicates the set of atoms neighbouring n , and E_{at} is the energy of an isolated neutral atom (Appendix B).

Consider possible hopping exponents $q^{\alpha\beta}$. The simplest choice is that all elements are equal, $q^{\alpha\beta} = q$. This has the advantage that the ground-state density matrix would be invariant to small changes in volume [2]. Moreover, the Hamiltonian would be separable into the outer product of orbital- and position-dependent parts, and so could be expressed on a basis in which the orbital part was diagonalised. We could write $\hat{H} = c_1 \mathbf{P}_1 \hat{h}(\{R\}) + c_2 \mathbf{P}_2 \hat{h}(\{R\})$, with $\mathbf{P}_1(\mathbf{P}_2)$ being a projector onto the first(second) eigenstate of the orbital part of the Hamiltonian and $c_1(c_2)$ the corresponding eigenvalue. Note that this separation is valid even if the electron–electron interactions given in Appendix B are included. However, we would find surprising unphysical consequences if we then performed time-dependent tight-binding (TD-TB). In TD-TB (a full description of which can be found in [10]) the evolution of the density matrix is given by the quantum Liouville equation $i\hbar \dot{\hat{\rho}} = [\hat{H}, \hat{\rho}]$. The density matrix can quite generally be written as $\hat{\rho} = \mathbf{P}_1 \rho \mathbf{P}_1 + \mathbf{P}_1 \rho \mathbf{P}_2 + \mathbf{P}_2 \rho \mathbf{P}_1 + \mathbf{P}_2 \rho \mathbf{P}_2$. As the projectors are time-invariant, we see immediately that the quantum Liouville equation would become $i\hbar d/dt(\mathbf{P}_a \hat{\rho} \mathbf{P}_b) = [\hat{H}, \mathbf{P}_a \hat{\rho} \mathbf{P}_b]$; we find that the projected parts of the density matrix would evolve independently. Since the trace of any matrix commutator is zero, $\text{Tr}(\mathbf{P}_a \hat{\rho} \mathbf{P}_b)$ is independent of time. The total occupation of each orbital (summed over lattice sites) would therefore remain constant.

The next simplest case for the hopping exponents \mathbf{q} is to fix them to different values. We can be guided by the physics of s–d-band mixing, and choose the exponents to match the s- and d-orbital exponents of Harrison’s TB model [11], $q^{ss} = 2$, $q^{ss^*} = q^{s^*s} = 7/2$, $q^{s^*s^*} = 5$. The s^* -orbital is therefore spherically symmetric like an s-orbital, but tails off rapidly like a d-orbital. We note that, while fitting to the cohesive energy, elastic constants and density of states, the absolute level of the first moment of the bands is immaterial, and only the difference $\Delta = E_s - E_{s^*}$ is important. The bandfilling is fixed to half-filled for the group VIIIb metals and three-quarters for the Ib metals. This gives a total of two or three electrons per atom, respectively, in the neutral state. Finally, we make the repulsive index p a floating point variable, giving a total of six parameters to fit $\{\epsilon, p, \Delta, \mathbf{c}\}$.

The six parameters are fitted to the following six empirical quantities: the equilibrium condition at the experimentally observed lattice parameter; the cohesive energy of the low temperature crystal; the three elastic moduli of the perfect fcc crystal and the density of states at the Fermi level as calculated using DFT with the Castep code [12]. This is done by least squares fitting. For a given choice $c^{\alpha\beta}$ and Δ , the lattice parameter and cohesive energy (from [13]) are fitted exactly by varying p and ϵ . This leaves a four-dimensional search to best fit the elastic properties and density of states. Candidate fits are discarded if they are mechanically unstable (any calculated elastic constant not positive, or $c_{11} < c_{12}$). They are also discarded if the body-centred cubic (bcc) structure is found to be more stable than the fcc. Finally, we discard any fit for which any point defect formation energy (Section 4) is unreasonably small or negative, as this also indicates an unstable potential.

The absolute values of E_s and E_{s^*} together with the on-site Coulomb repulsion energy U can then be fit for the electron affinity and first ionisation potential (Appendix B).

3. Potentials for fcc transition metals

The parameterisation of the best-fit potentials found is given in Table 1. The elastic constants and the electronic properties, including the density of states at the Fermi level computed as part of the fitting process, are given in Table 2.

It is seen that a reasonable fit to all three elastic constants can be achieved with this simple model. Only c_{44} for gold is poor. Candidate fits for gold with a much better match for c_{44} were rejected on the grounds of unacceptable point defect energies. It can be seen that the densities of states at E_F can be well reproduced by tuning the parameters of this simple model. This is encouraging, but inspection of histograms of the densities of states shows that the fit to the electronic structure is good not just at E_F , but in a window centred on it (Figure 1). Best fitting to the elastic properties and the density of states at E_F has naturally produced a wide flat s-band with a sharply peaked s*-band superposed on it. The bandfilling has ensured that the s* peak appears either at, or 2 eV below, E_F . The coincidence of true and model densities of states around the Fermi energy implies that where transport or electronic excitation phenomena probe the d-band in a real metal, a similar bandstructure effect might be seen with the model potential at roughly the same energy scale.

Table 1. Parameterisation of the potentials.

	a	ϵ	p	E_s	E_{s^*}	c_{ss}	c_{ss^*}	$c_{s^*s^*}$	U
Cu	3.61	8.340E-04	13.7723	-4.4800	-4.5070	1970.6920	-2.5959	120.8204	6.493
Ag	4.09	1.790E-04	17.1865	-4.4501	-4.4411	7303.9667	894.0779	0.3231	6.270
Au	4.08	2.270E-04	17.5275	-5.7873	-5.7682	6726.0558	1707.7570	0.8968	6.914
Ni	3.523	4.080E-03	11.2761	-4.7125	-4.0878	543.9727	53.2842	0.7294	5.854
Pd	3.887	6.620E-04	15.4687	-4.4483	-4.4484	1889.9262	641.9126	161.8567	7.777
Pt	3.924	6.800E-03	11.9395	-5.7544	-5.3872	220.5027	138.7442	78.4589	6.525

Note: a is in Å and ϵ , E_s , E_{s^*} , U are measured in eV.

Table 2. Elastic constants measured in eV/Å³, and electronic properties of the perfect crystal for the potentials fitted here.

	c_{11}	c_{12}	c_{44}	E_b	E_f	E_t	$D(E_f)$	ν
Cu	1.068 (1.100)	0.832 (0.780)	0.523 (0.510)	-29.143	-2.054	0.453	0.101 (0.118)	0.750
Ag	0.834 (0.869)	0.622 (0.604)	0.394 (0.344)	-24.740	-2.418	-0.324	0.125 (0.117)	0.750
Au	1.207 (1.314)	0.897 (0.975)	0.568 (0.274)	-31.838	-3.023	-0.295	0.130 (0.119)	0.750
Ni	1.595 (1.630)	1.098 (0.940)	0.740 (0.820)	-38.705	-4.085	2.187	1.753 (1.693)	0.500
Pd	1.609 (1.460)	1.016 (1.100)	0.642 (0.440)	-28.133	-4.443	0.751	0.919 (1.083)	0.500
Pt	2.250 (2.230)	1.556 (1.585)	0.452 (0.480)	-48.577	-5.512	4.871	0.999 (0.915)	0.500

Note: The experimental values for elastic constants are in parentheses from [13]. The Fermi level (E_F) and band edges (E_b , E_t) of the model are given in eV. The density of states at the Fermi level is in states per atom per eV, with the DFT calculated value in parentheses. ν is the total s, and s* bandfilling used.

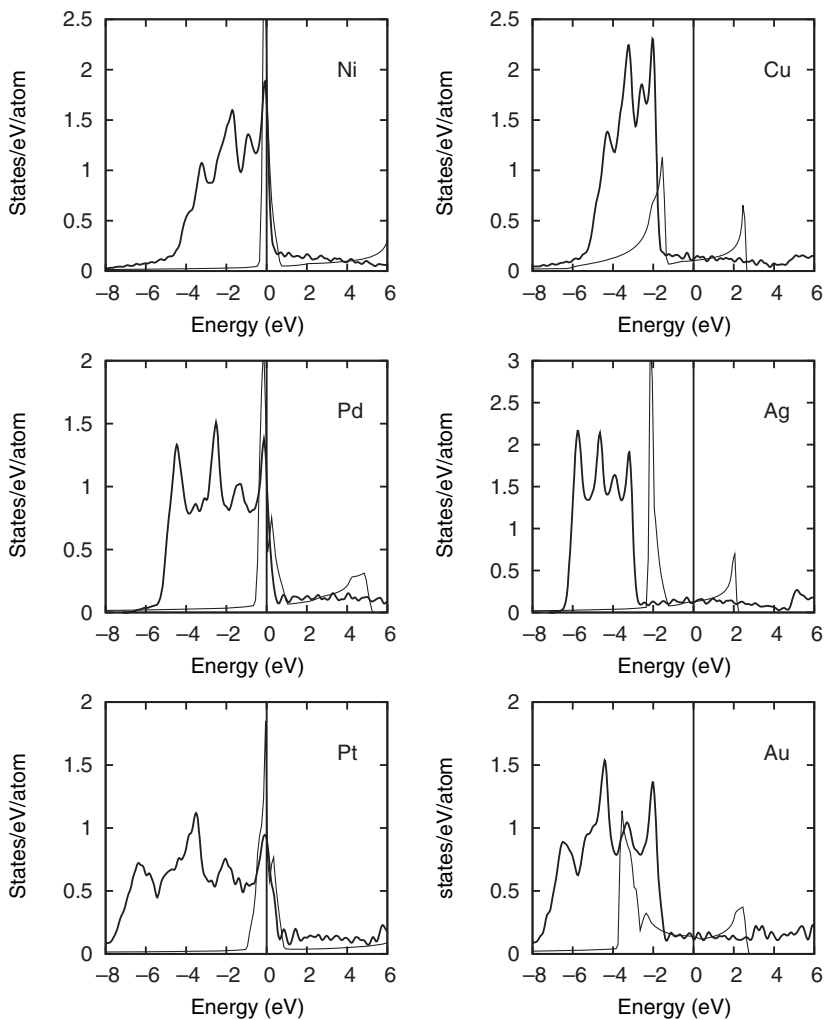


Figure 1. Computed densities of states around the Fermi level for group Ib and VIIIb elements. The energy scales are shifted so that the Fermi level is adjusted to zero. In each plot, the dark line has been computed with the DFT code Castep [12], and the lighter line using the simple model parameterisations given here. At the Fermi level, all three Ib elements are seen to have a very flat density of states, which is reproduced by our simple model. We note that the s^* -band also produces a spike in the density of states about 2eV below the Fermi level. The three VIIIb elements are characterised by having a rapidly falling density of states at the Fermi level, which is reproduced by our simple model. Note that our parameterisation for nickel is spin-degenerate.

4. Point defect energies

As a test of the transferability of the potentials produced, we have computed point defect formation energies at $T=0$ K. The values quoted in Table 3 are relaxed constant-volume point defect formation energies for vacancies, and self-interstitials, computed using a simulation cell of $6 \times 7 \times 8$ fcc unit cells

Table 3. Calculated point defect energies at $T=0\text{K}$, for the vacancy, and three self-interstitial types ($\langle 100$ -split dumbbell, octahedral and tetrahedral).

	H_f^{vac}	$H_f^{(100)}$	H_f^{oct}	H_f^{tet}
Cu	0.62 (1.04–1.31) [1.33a] {0.60}	4.77 {2.51}	4.36 {2.78}	5.81 {3.16}
Ag	0.60 (1.09–1.19) [1.24a] {0.57}	5.61 {3.79}	5.28 {3.90}	6.89 {4.68}
Au	0.54 (0.89–1.00) [0.82a] {0.30}	7.63 {3.02}	7.25 {6.52}	9.32 {3.10}
Ni	1.06 (1.45–1.80) [1.77a]	5.04 [4.07b]	5.10 [4.25b]	6.27 [4.69b]
Pd	1.09 (1.60–2.10) [1.70c]	6.59	6.71	8.36
Pt	0.87 (1.15–1.60) [1.16c]	6.17	6.35	7.55

Notes: ^aKorhonen et al. [14].

^bTucker et al. [15].

^cMattsson and Mattsson [16].

All energies reported in eV. The experimental results are given in round parentheses. DFT results are in square braces where available. The results generated with the TB model of Ref. [2] using the same procedure as that outlined in the text given in curly braces.

(totalling 1344 ± 1 atoms). An on-site Coulomb correlation energy is included in these calculations (Appendix B). We see from Table 3 that the $\langle 100$ -split dumbbell is the lowest energy interstitial for the group VIIIb metals, in line with other studies. The noble metals show the octohedral self-interstitial to be the lowest energy configuration, whereas it is usually believed to be the $\langle 100$ -split [17]. This indicates a failure of the simple model – the potential forms given here are too stiff at short distances, as indicated by the rather high index p in the repulsive part of the potential. It is also notable that the s-band models underestimate the vacancy formation energies by about a factor of 2.

5. Conclusion

Where a dynamical process in a metal requires an explicit treatment of the electrons, a compromise must always be made between the realism of a simulation in terms of its duration, size and the accuracy of the electronic Hamiltonian. This will remain true regardless of advances in computational power and algorithms. We have developed a simplified TB model for the simulation of large metallic systems where an explicit treatment of electron dynamics is essential. The model builds on an earlier single s-band TB model, and improves it by returning a more accurate density of states at the Fermi level and integer electronic occupancies of neutral atoms.

The elastic properties are well reproduced. The electronic density of states 1 eV either side of the Fermi level is reproduced reasonably well in all cases, suggesting that these models may also be suited to studying current-induced effects in nanowires. The density of states for the model noble metals show a large spike 2 eV below the Fermi level, around the same position as the real d-band edge. The model is a significant improvement on the earlier s-band model of [2] and will enable further qualitative insight to be gained into complex dynamical processes involving electronic excitation in metals.

Acknowledgements

The authors would like to thank Mike Finnis, Andrew Horsfield, Chris Race and Tchavdar Todorov for their constructive criticism in the formulation and assessment of this model. Calculations were performed on Hector and IC-HPC. D.R. Mason was supported by EPSRC grant number EP/C524403.

References

- [1] D.A. Papaconstantopoulos and M.J. Mehl, *J. Phys. Condens. Matter* 15 (2003) p.R413.
- [2] A.P. Sutton, T.N. Todorov, M.J. Cawkwell and J. Hoekstra, *Phil. Mag. A* 81 (2001) p.1833.
- [3] T.N. Todorov, J. Hoekstra and A.P. Sutton, *Phys. Rev. Lett.* 86 (2001) p.3606.
- [4] E.J. McEniry, D.R. Bowler, D. Dundas, A.P. Horsfield, C.G. Sánchez and T.N. Todorov, *J. Phys. Condens. Matter* 19 (2007) p.196201.
- [5] J. le Page, D.R. Mason, C.P. Race and W.M.C. Foulkes, *New J. Phys.* 11 (2009) p.013004.
- [6] C.P. Race, D.R. Mason and A.P. Sutton, *J. Phys. Condens. Matter* 21 (2009) p.115702.
- [7] W.P. Su, J.R. Schrieffer and A.J. Heeger, *Phys. Rev. Lett.* 42 (1979) p.1698.
- [8] D.G. Pettifor, *Bonding and Structure of Molecules and Solids*, Oxford University Press, Oxford, 1995.
- [9] P. Vogl, H.P. Hjalmarson and J.D. Dow, *J. Phys. Chem. Solid.* 44 (1983) p.365.
- [10] T.N. Todorov, *J. Phys. Condens. Matter* 13 (2001) p.10125.
- [11] W.A. Harrison, *Elementary Electronic Structure*, World Scientific Publishing, Singapore, 1999.
- [12] S.J. Clark, M.D. Segall, C.J. Pickard, P.J. Hasnip, M.J. Probert, K. Refson and M.C. Payne, *Zeitschr. Kristall.* 220 (2005) p.567.
- [13] G. Simmons and H. Wang, *Single Crystal Elastic Constants and Calculated Aggregate Properties: A Handbook*, MIT Press, Cambridge, MA, 1971.
- [14] T. Korhonen, M.J. Puska and R.M. Nieminen, *Phys. Rev. B* 51 (1995) p.9256.
- [15] J.D. Tucker, T.R. Allen and D. Morgan, *Ab initio defect properties for modeling radiation-induced segregation in Fe–Ni–Cr alloys*, in *Proceedings of the 13th International Symposium on Environmental Degradation of Materials in Nuclear Power Systems*, Whistler, BC, Canada, August 2007.
- [16] T.R. Mattsson and A.E. Mattsson, *Phys. Rev. B* 66 (2002) p.214110.
- [17] W. Schilling, *J. Nucl. Mater.* 69&70 (1978) p.465.
- [18] D.R. Lide (ed.), *CRC Handbook of Chemistry and Physics*, 84th ed., Section 10, CRC Press, Boca Raton, FL, 2003.

Appendix A: Polynomial tails

We want an order n polynomial truncation function $p_n(r)$ in the interval $r_t \leq r \leq r_c$ which can smoothly take a function $f(r)$ and its first m derivatives to zero at a cutoff point $r = r_c$. For a transferable polynomial, we apply the truncation function in a multiplicative fashion, that is, we replace the bare function $f(r)$ with

$$\tilde{f}(r) = \begin{cases} f(r) & r \leq r_t \\ f(r)p_n(r) & r_t \leq r \leq r_c \\ 0 & r \geq r_c \end{cases} \quad (\text{A1})$$

Table A1. First few truncation functions for smooth polynomial tails.

m	a											
	0	1	2	3	4	5	6	7	8	9	10	11
0	0	1										
1	0	0	3	-2								
2	0	0	0	10	-15	6						
3	0	0	0	0	35	-84	70	-20				
4	0	0	0	0	0	126	-420	540	-315	70		
5	0	0	0	0	0	0	462	-1980	3465	-3080	1386	-252

The purpose of such a termination is to remove the discontinuities in such a function which can violate conservation laws during numerical integration. We can therefore identify that m needs to be at least the order of the integrator, and that the number of derivatives matched at r_i should also be m . The lowest order polynomial that will meet the boundary conditions is then $n = 2m + 1$.

It is convenient to write $x = \frac{r_c - r}{r_c - r_i}$, and use the function $\tilde{p}_n(x) = \sum_{i=0}^n a_i x^i$. The matching conditions take the form of a set of simultaneous equations which can be solved to give the coefficients a_i . The boundary conditions at $r = r_i, x = 0$ give $a_i = 0$ for $i \leq m$. The boundary conditions at $r = r_c, x = 1$ give the set of simultaneous equations

$$\begin{pmatrix} 1 & 1 & \dots & 1 \\ m+1 & m+2 & \dots & 2m+1 \\ (m+1)(m) & (m+2)(m+1) & \dots & (2m+1)(2m) \\ \dots & \dots & \dots & \dots \\ (m+1)!/1! & (m+2)!/2! & \dots & (2m+1)!/(m+1)! \end{pmatrix} \begin{pmatrix} a_{m+1} \\ a_{m+2} \\ a_{m+3} \\ \dots \\ a_{2m+1} \end{pmatrix} = \begin{pmatrix} 1 \\ 0 \\ 0 \\ \dots \\ 0 \end{pmatrix},$$

where the first row fixes $\tilde{p}_n(x = 1) = 1$, and the subsequent m rows zero the first m derivatives at $x = 1$.

The first few solutions are given in Table A1. Note that each truncation function $\tilde{p}_n(x)$ is symmetric about $x = \frac{1}{2}$.

Appendix B: On-site Coulomb correlation energy

The energy of isolated charged ions may be written down by the inspection of Hamiltonian and bandfilling. With ionic charge Q (measured in units of electronic charge, so that an excess of one electron gives $Q = -1$) relative to the neutral atom we add to the on-site Hamiltonian elements an additional term $-UQ$ to represent the on-site Coulomb correlation energy for a spin-degenerate system (U is analogous to the Hubbard energy in non-spin-degenerate systems). For an isolated atom, the Hamiltonian is then

$$H = \begin{pmatrix} E_s - UQ & 0 \\ 0 & E_{s^*} - UQ \end{pmatrix}, \tag{B1}$$

and the energy of the non-interacting ion is $E_{ai}(Q) = 2E_s \rho_{ss} + 2E_{s^*} \rho_{s^*s^*} + \frac{1}{2} UQ^2$. Note that the factor of one half is needed to avoid double-counting the electrons. The energy of the ionic charge states is given in Table A2. The energy scale U and the lower of E_s and E_{s^*} are fitted to reproduce exactly the first ionisation potential I_1 and the electron affinity I_a , making this parameterisation suitable for sputtered ions as well as those in the bulk. These values are then given in Table A3. We note that our simple model underestimates the second ionisation energy.

Note that the value of U does not affect equilibrium properties of the metal, such as cohesive energy or elastic constants, as all atoms are then neutral. In any dynamic process, ionic charges are screened by mobile electrons, which can be accounted for more fully by supplementing the present model with the addition of a pairwise Coulombic interaction.

Table A2. The energy of non-interacting ions.

Charge state Q	$\nu = \frac{1}{2}$ (Ni, Pd, Pt)		$\nu = \frac{3}{4}$ (Cu, Ag, Au)	
	$E_s < E_{s^*}$	$E_s \geq E_{s^*}$	$E_s < E_{s^*}$	$E_s \geq E_{s^*}$
-1	$2E_s + E_{s^*} + \frac{1}{2}U$	$2E_{s^*} + E_s + \frac{1}{2}U$	$2E_s + 2E_{s^*} + \frac{1}{2}U$	$2E_{s^*} + 2E_s + \frac{1}{2}U$
0	$2E_s$	$2E_{s^*}$	$2E_s + E_{s^*}$	$2E_{s^*} + E_s$
+1	$E_s + \frac{1}{2}U$	$E_{s^*} + \frac{1}{2}U$	$2E_s + \frac{1}{2}U$	$2E_{s^*} + \frac{1}{2}U$
+2	$2U$	$2U$	$E_s + 2U$	$E_{s^*} + 2U$
I_a	$-E_{s^*} - \frac{1}{2}U$	$-E_s - \frac{1}{2}U$	$-E_{s^*} - \frac{1}{2}U$	$-E_s - \frac{1}{2}U$
I_1	$-E_s + \frac{1}{2}U$	$-E_{s^*} + \frac{1}{2}U$	$-E_{s^*} + \frac{1}{2}U$	$-E_s + \frac{1}{2}U$
I_2	$-E_s + \frac{3}{2}U$	$-E_{s^*} + \frac{3}{2}U$	$-E_s + \frac{3}{2}U$	$-E_{s^*} + \frac{3}{2}U$

Notes: The energy of the isolated neutral ion required by Equation (4) is given in the row for $Q=0$. The electron affinity and first two ionisation energies (I_a and I_1, I_2) are also given.

Table A3. Ionic properties of the atoms.

	E_{at}	I_a	I_1	I_2
Cu	-13.494	1.233	7.727	14.25 (20.30)
Ag	-13.341	1.306	7.576	13.86 (21.46)
Au	-17.343	2.311	9.225	16.16 (20.53)
Ni	-9.425	1.161	7.639	13.49 (18.18)
Pd	-8.897	0.560	8.337	16.11 (19.39)
Pt	-11.509	2.125	9.017	15.54 (18.57)

Notes: All energies are given in eV. The electron affinity and first ionisation potential (I_a and I_1 , respectively) are fitted exactly to the experimental values from [18]. The second ionisation potential is compared to the experimental value in parentheses.